A Rational Chemical Intervention Strategy To Circumvent Bioactivation Liabilities Associated with a Nonpeptidyl Thrombopoietin Receptor Agonist Containing a 2-Amino-4-arylthiazole...

ARTICLE *in* CHEMICAL RESEARCH IN TOXICOLOGY · DECEMBER 2007

Impact Factor: 3.53 · DOI: 10.1021/tx700270r · Source: PubMed

A Rational Chemical Intervention Strategy To Circumvent Bioactivation Liabilities Associated with a Nonpeptidyl Thrombopoietin Receptor Agonist Containing a 2-Amino-4-arylthiazole Motif

Amit S. Kalgutkar,* James Driscoll, Sabrina X. Zhao, Gregory S. Walker, Richard M. Shepard, John R. Soglia, James Atherton, Linning Yu, Abdul E. Mutlib, Michael J. Munchhof, Lawrence A. Reiter, Christopher S. Jones, Johnathan L. Doty, Kristen A. Trevena, Christopher L. Shaffer, and Sharon L. Ripp

Pharmacokinetics, Dynamics and Metabolism Department, Pfizer Global Research and Development, Groton, Connecticut 06340, and Ann Arbor, Michigan 48105

Received July 26, 2007

The current study examined the bioactivation potential of a nonpeptidyl thrombopoietin receptor agonist, 1-(3-chloro-5-((4-(4-fluoro-3-(trifluoromethyl)phenyl)thiazol-2-yl)carbamoyl)pyridine-2-yl)piperidine-4-carboxylic acid (**1**), containing a 2-carboxamido-4-arylthiazole moiety in the core structure. Toxicological risks arising from P450-catalyzed C4–C5 thiazole ring opening in **1** via the epoxidation → diol sequence were alleviated, since mass spectrometric analysis of human liver microsome and/or hepatocyte incubations of **1** did not reveal the formation of reactive acylthiourea and/or glyoxal metabolites, which are prototypic products derived from thiazole ring scission. However, 4-(4-fluoro-3-(trifluoromethyl)phenyl)thiazol-2-amine (**2**), the product of hydrolysis of **1** in human liver microsomes, hepatocytes, and plasma, underwent oxidative bioactivation in human liver microsomes, since trapping studies with glutathione led to the formation of two conjugates derived from the addition of the thiol nucleophile to **2** and a thiazole-*S*-oxide metabolite of **2**. Mass spectral fragmentation and NMR analysis indicated that the site of attachment of the glutathionyl moiety in both conjugates was the C5 position in the thiazole ring. Based on the structures of the glutathione conjugates, two bioactivation pathways are proposed, one involving β-elimination of an initially formed hydroxylamine metabolite and the other involving direct two-electron oxidation of the electron-rich 2-aminothiazole system to electrophilic intermediates. This mechanistic insight into the bioactivation process allowed the development of a rational chemical intervention strategy that involved blocking the C5 position with a fluorine atom or replacing the thiazole ring with a 1,2,4-thiadiazole group. These structural changes not only abrogated the bioactivation liability associated with **1** but also resulted in compounds that retained the attractive pharmacological and pharmacokinetic attributes of the prototype agent.

Introduction

Thrombopoietin (Tpo),[1] a cytokine that is produced primarily in the liver, is a glycoprotein consisting of 332 amino acids that regulates platelet production by stimulating proliferation and differentiation of hematopoietic stem cells, megakaryocytic progenitor cells, and megakaryocytes (*1, 2*). Upon binding to its receptor, Tpo activates Janus kinase 2, which leads to activation of mitogen-activated protein kinase pathways to drive cell proliferation and differentiation (*3–5*). While absence of Tpo leads to thrombocytopenia, administration of recombinant Tpo to rodents and humans leads to significant increases in circulating levels of platelets (*6–9*). Consequently, recombinant human Tpo has been clinically evaluated for treatment of thrombocytopenia patients, including those undergoing nonmyeloablative chemotherapy (*10*). Considering the usual difficulties associated with protein-based therapeutics, such as inconvenient routes of administration, an orally bioavailable nonpeptidyl Tpo receptor agonist may be more beneficial to patients suffering from thrombocytopenia. Consequently, the identification of small-molecule agonists of the Tpo receptor has been an active area of research, and several nonpeptidyl agonists have been reported in recent years (*11–14*). In our ongoing effort to identify novel Tpo mimics, we have characterized a series of piperidine-4-carboxylic acids exemplified by 1-(3-chloro-5-((4-(4-fluoro-3-(trifluoromethyl)phenyl)thiazol-2-yl)carbamoyl)pyridine-2-yl)piperidine-4-carboxylic acid (**1**) (Scheme 1) as selective, nonpeptidyl agonists of the Tpo receptor. Compound **1** exhibited an EC_{50} value of 99 nM when tested in vitro for its ability to induce proliferation of the murine Ba/F3-hTpoR hematopoietic cell line, which expresses the human Tpo receptor (*15*).

* To whom correspondence should be addressed. Tel: (860) 715-2433. Fax: (860) 686-1059. E-mail: amit.kalgutkar@pfizer.com.

[1] Abbreviations: Tpo, thrombopoietin; **1**, 1-(3-chloro-5-((4-(4-fluoro-3-(trifluoromethyl)phenyl)thiazol-2-yl)carbamoyl)pyridine-2-yl)piperidine-4-carboxylic acid; **2**, 4-(4-fluoro-3-(trifluoromethyl)phenyl)thiazol-2-amine; **3**, 6-(4-carboxypiperidin-1-yl)-5-chloronicotinic acid; ANFT, 2-amino-4-(5-nitro-2-furyl)thiazole; **4**, 1-(3-chloro-5-((5-fluoro-4-(4-fluoro-3-(trifluoromethyl)phenyl)thiazol-2-yl)carbamoyl)pyridine-2-yl)piperidine-4-carboxylic acid; **5**, 1-(3-chloro-5-((3-(4-fluoro-3-(trifluoromethyl)phenyl)-1,2,4-thiadiazol-5-yl)carbamoyl)pyridine-2-yl)piperidine-4-carboxylic acid; **6**, 5-fluoro-4-(4-fluoro-3-(trifluoromethyl)phenyl)thiazol-2-amine; **7**, 3-(4-fluoro-3-(trifluoromethyl)phenyl)-1,2,4-thiadiazol-5-amine; LC–MS/MS, liquid chromatography–tandem mass spectrometry; CID, collision-induced dissociation; SPE, solid-phase extraction; C_{max}, peak plasma concentration; t_{max}, time of C_{max}; CL_p, plasma clearance; AUC, area under the plasma concentration–time curve; *F*, relative oral bioavailability; NSAID, nonsteroidal anti-inflammatory drug.

10.1021/tx700270r CCC: $37.00
Published on Web 10/13/2007

Scheme 1. Proposed Mechanism of Bioactivation of the Nonpeptidyl Thrombopoietin Receptor Agonist 1

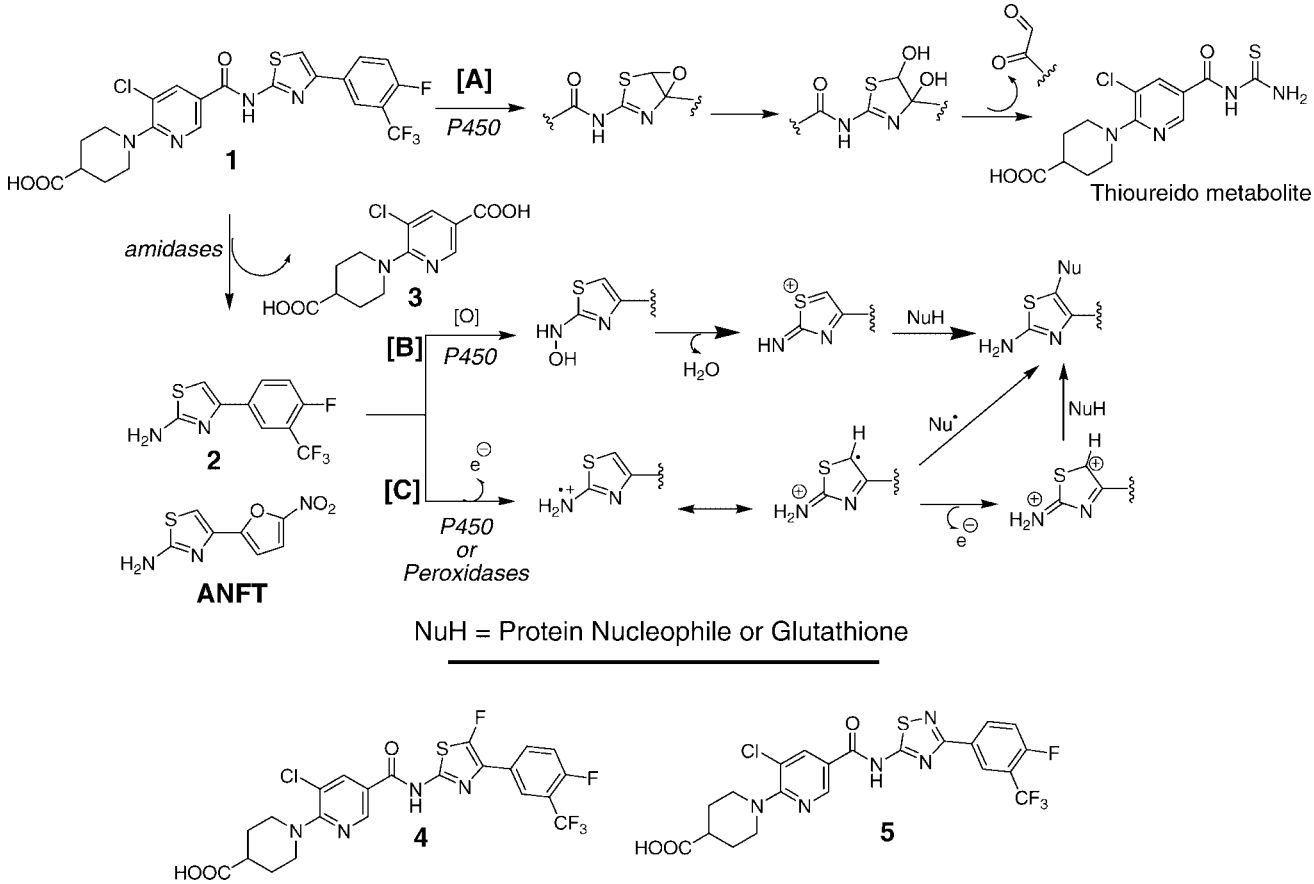

Given the increasing evidence linking toxicity to drug bioactivation (*16–18*), it is important to identify and minimize metabolic activation liabilities as early as possible in the overall drug discovery process. In this context, the presence of the 2-carboxamido-4-arylthiazole motif in **1** represented a significant concern, considering the susceptibility of this substituent to thiazole ring opening via the C4–C5 epoxidation → diol pathway, leading to formation of acylthiourea and/or glyoxal metabolites, as depicted in Scheme 1, pathway A (*19*). Once formed, thioureas can undergo S-oxidation to electrophilic sulfenic acid derivatives capable of oxidizing or forming adducts with critical biomacromolecules or GSH (*20–22*). In addition, amide bond hydrolysis in **1** under physiological conditions could potentially liberate 4-(4-fluoro-3-(trifluoromethyl)phenyl)thiazol-2-amine (**2**), which can undergo bioactivation via one or both of two pathways: (a) β-elimination of water from an initially formed hydroxylamine metabolite to yield an electrophilic intermediate capable of reacting with nucleophiles (Scheme 1, pathway B) in a manner similar to that observed with nitroheteroaromatics such as ronidazole and metronidazole following their reductive bioactivation (*23*) and (b) direct one- or two-electron oxidation of the electron-rich 2-aminothiazole motif by P450 or peroxidases (Scheme 1, pathway C), as has been demonstrated with the bladder carcinogen 2-amino-4-(5-nitro-2-furyl)thiazole (ANFT, Scheme 1) (*24, 25*).

The purpose of the present study was to examine the in vitro bioactivation potential of **2**, the product of hydrolysis of **1**, in human hepatic tissue. Initial stability examination in human liver microsomes, cryopreserved human hepatocytes, and/or plasma revealed that the carboxamide linkage in **1** underwent enzymatic hydrolysis, liberating **2** as a metabolite. Incubation of a synthetic standard of **2** with GSH-supplemented human liver microsomes led to the NADPH-dependent formation of two GSH conjugates. Mass spectral and ^{1}H NMR analysis established the C5 position on the thiazole ring as the site of attachment of the glutathionyl moiety, consistent with the hypothesis proposed in pathway B and/or C of Scheme 1. On the basis of this information, we devised a rational chemical intervention strategy that led to the synthesis of the C5 fluoro and thiadiazole analogues **4** and **5** (see Scheme 1), respectively, as compounds that should not be susceptible to the bioactivation pathway presented in Scheme 1. Compounds **4** and **5** were found to retain Tpo receptor agonist properties and the otherwise attractive pharmacokinetic attributes of **1**. Importantly, the products of the hydrolysis of the Tpo agonists **4** and **5**, namely, 5-fluoro-4-(4-fluoro-3-(trifluoromethyl)phenyl)thiazol-2-amine (**6**) and 3-(2-fluoro-3-(trifluoromethyl)phenyl-1,2,4-thiadiazol-5-amine (**7**), respectively, were devoid of the bioactivation liability associated with **2**.

Experimental Procedures

Chemicals. Piperidine-4-carboxylic acid analogues **1**, **4**, and **5** were synthesized and purified at Pfizer Global Research and Development (Groton, CT) (*26, 27*). 2-(4-Fluoro-3-(trifluoromethyl)phenyl)-2-oxoacetaldehyde was synthesized according to the method of Paul et al. (*28*). Chemical yields are unoptimized specific examples of one preparation. Chemicals and reagents used in synthesis and 4-phenyl-1*H*-imidazol-2-amine were purchased from Aldrich (Milwaukee, WI). Isocitric acid dehydrogenase, $MgCl_2$, DL-isocitric acid, $NADP^+$, catalase (2950 units/mg), desferoxamine mesylate, 30% hydrogen peroxide, and GSH were obtained from Sigma-Aldrich (Milwaukee, WI). Cryopreserved human hepatocytes were purchased from In Vitro Technologies, Inc. (IVT, Baltimore, MD). Human liver microsomal fractions pooled from 53 individual donors were purchased from BD Gentest (Woburn, MA).

4-(4-Fluoro-3-(trifluoromethyl)phenyl)thiazol-2-amine (2). 4-Fluoro-3-(trifluoromethyl)acetophenone (175 mmol) and sulfuryl chloride (350 mmol) were added to a 500 mL reaction vessel, and the

reaction mixture was concentrated to dryness. Ethanol (250 mL) and thiourea (180 mmol) were added to the resulting residue. The reaction mixture was then refluxed at 90 °C for 24 h. Subsequent concentration yielded a residue that was suspended in $CHCl_3$ (500 mL) and washed twice with saturated $NaHCO_3$ (250 mL). The organic layer was dried over sodium sulfate, filtered, and concentrated. The product was triturated twice with hexanes (400 mL) and decanted to afford the desired product as an off-white solid in 74% yield (34.2 g). Electrospray ionization analysis in the positive ion mode revealed a single peak (t_R = 13.3 min) with a molecular ion ($M + H^+$) at *m/z* 263 and a base fragment at *m/z* 152. ^{1}H NMR ($CDCl_3$): δ 7.32 (t, 1 H, ArH), 8.06 (m, 1 H, ArH), 8.10 (m, 1 H, ArH).

6-(4-Carboxypiperidin-1-yl)-5-chloronicotinic Acid (3). Step 1. 6-(4-(Ethoxycarbonyl)piperidin-1-yl)-5-chloropyridine-3-carboxylic Acid. 5,6-Dichloronicotinic acid (7.68 g, 0.04 mmol), anhydrous dioxane (200 mL), ethyl piperidine-4-carboxylate (12.6 g, 0.08 mmol), and potassium hydrogen phosphate (17.4 g, 0.1 mol) were added to a 1000 mL large-neck round-bottom flask, and the reaction mixture was stirred at reflux (100 °C) overnight. Upon cooling, the mixture was filtered to remove most of the potassium salts, and the filtrate was concentrated. Flash column chromatography (Isco CombiFlash 330 g, RediSep cartridge) using a 2–10% methanol/$CHCl_3$ solvent system afforded the desired product as a yellow-white powder (6.75 g). **Step 2. 6-(4-Carboxypiperidin-1-yl)-5-chloronicotinic Acid (3).** A reaction mixture containing 6-(4-(ethoxycarbonyl)piperidin-1-yl)-5-chloropyridine-3-carboxylic acid (150 mg, 0.5 mmol) and 1 N LiOH (~1.5 mL) in MeOH (3 mL) was stirred at room temperature for 4 h. The reaction mixture was diluted with water, extracted with ethyl acetate (2 × 10 mL; the organic washing was discarded), acidified with 1 N HCl, and extracted with ethyl acetate (2 × 20 mL). The combined organic solution was washed with water (2 × 20 mL), dried with $MgSO_4$, and filtered, and the solvent was removed in vacuo. Flash column chromatography (Isco CombiFlash 330 g, RediSep cartridge) using a 2–10% methanol/$CHCl_3$ solvent system afforded the desired product as an off-white powder (130 mg, 95%). Electrospray ionization analysis in the positive ion mode revealed a single peak (t_R = 9.7 min) with a molecular ion ($M + H^+$) at *m/z* 285 and a base fragment at *m/z* 185. ^{1}H NMR (DMSO-d_6): δ 8.65 (d, 1 H, ArH), 8.10 (d, 1 H, ArH), 3.93 (d, 2 H, CH_2), 2.98 (t, 2 H, CH_2), 2.46 (m, 1 H, CH), 1.89 (d, 2 H, CH_2), 1.61 (q, 2 H, CH_2).

5-Fluoro-4-(4-fluoro-3-(trifluoromethyl)phenyl)thiazol-2-amine (6). Selectfluor (16.0 g, 44.5 mmol) was added to a stirred suspension of 4-(4-fluoro-3-(trifluoromethyl)phenyl)thiazol-2-amine (10.49 g, 40.0 mmol) in anhydrous acetonitrile (200 mL) at 0 °C. The reaction mixture was allowed to warm to room temperature overnight. The solvent volume was reduced in vacuo, and then the solution was diluted with dichloromethane (150 mL). The precipitated quinuclidine salts were removed by vacuum filtration, and the combined filtrate and organic washes were preadsorbed onto silica gel and chromatographed (Isco CombiFlash 330 g, RediSep cartridge) using 5–55% ethyl acetate in hexanes for 1 h. Fractions containing product were pooled, evaporated, and dried under high vacuum to afford the desired product as a pinkish crystalline solid (4.96 g, 41.8%). Electrospray ionization analysis in the positive ion mode revealed a single peak (t_R = 15.1 min) with a molecular ion ($M + H^+$) at *m/z* 281 and a base fragment at *m/z* 219. ^{1}H NMR ($CDCl_3$): δ 7.02 (t, 1 H, ArH), 7.64 (m, 1 H, ArH), 7.85 (m, 1 H, ArH).

3-(4-Fluoro-3-(trifluoromethyl)phenyl)-1,2,4-thiadiazol-5-amine (7). A solution of 4-fluoro-3-trifluoromethylbenzonitrile (10 g, 52.9 mmol) and sodium methoxide (10.6 mL of a 0.5 M solution in methanol, 5.3 mmol, 0.1 equiv) in methanol (40 mL) was allowed to stir for 12–36 h at room temperature. Acetic acid (0.32 g, 5.3 mmol) and ammonium chloride (2.8 g, 52.9 mmol) were added in succession. The reaction mixture was stirred at 50 °C for 24 h and then cooled. The unreacted ammonium chloride was removed by filtration, and the resultant white solid (6 g, 24.8 mmol) was dissolved in methanol (50 mL). The solution was cooled to −5 °C and maintained at this temperature during the somewhat exothermic additions of bromine (3.96 g, 24.8 mmol) over a period of 5 min and potassium thiocyanate (2.4 g, 24.8 mmol) over a period of 1 min. To this mixture was added a solution of sodium methoxide in methanol [freshly prepared from sodium (1.14 g, 49.6 mmol) and methanol (30 mL)], resulting in the formation of a white precipitate. The reaction mixture was allowed to warm to room temperature and then was stirred for 3 h. The solution was concentrated to one-third of its original volume and poured into water (150 mL), resulting in the formation of a different white precipitate. This mixture was allowed to stir for 1 h, after which the precipitate was collected by filtration to provide 3.5 g (53%) of the title compound as a white solid. Electrospray ionization analysis in the positive ion mode revealed a single peak (t_R = 13.9 min) with a molecular ion ($M + H^+$) at *m/z* 264 and a base fragment at *m/z* 222.

1-(3-Chloro-5-(thioureidocarbonyl)pyridin-2-yl)piperidine-4-carboxylic Acid. Step 1. Ethyl 1-(5-(Chlorocarbonyl)piperidin-1-yl)-5-chloropyridine-3-carboxylic Acid. A reaction mixture containing 6-(4-(ethoxycarbonyl)piperidin-1-yl)-5-chloropyridine-3-carboxylic acid (4.66 g, 14.9 mmol) in dichloromethane (120 mL) was treated with thionyl chloride (7.09 g, 59.6 mmol). The mixture was warmed to 45 °C with stirring for 90 min. The solvent and any excess reagent were evaporated in vacuo, and the resulting residue was dried under high vacuum to afford the desired product as a yellow semisolid in 100% yield (5.35 g). Electrospray ionization analysis in the positive ion mode revealed a single peak (t_R = 2.88 min) with a molecular ion ($M + H^+$) at *m/z* 327. **Step 2. Ethyl 1-(3-Chloro-5-(thioureidocarbonyl)pyridin-2-yl)piperidine-4-carboxylate.** The procedure was adapted from a previously published protocol for the synthesis of *N*-benzoylthioureas (*29*). Ethyl 1-(5-(chlorocarbonyl)piperidin-1-yl)-5-chloropyridine-3-carboxylic acid (266 mg, 0.74 mmol), ammonium thiocyanate (85 mg, 1.11 mmol), polyethylene glycol-400 (13 mg), and anhydrous dichloromethane (2.0 mL) were added to a flame-dried flask. The reaction mixture was stirred for 1 h at room temperature, and then tris(hydroxymethyl)aminomethane (99 mg, 0.81 mmol) was added. After it was stirred for an additional 48 h at room temperature, the mixture was filtered to remove inorganic salts, and the solvent was concentrated in vacuo. The resulting solid was recrystallized from anhydrous ethanol to provide the desired product as a pale yellow solid (120 mg, 41%). Electrospray ionization analysis in the positive ion mode revealed a single peak (t_R = 2.9 min) with a molecular ion ($M + H^+$) at *m/z* 371. **Step 3. 1-(3-Chloro-5-(thioureidocarbonyl)pyridin-2-yl)piperidine-4-carboxylic Acid.** Ethyl 1-(3-chloro-5-(thioureidocarbonyl)pyridin-2-yl)piperidine-4-carboxylate (117 mg, 0.29 mmol) was stirred in 1:1 trifluoroacetic acid/dichloromethane (2 mL) for 72 h at room temperature. The solvent was concentrated in vacuo, and the oily residue was triturated with dichloromethane/hexanes to afford a pale yellow solid (95 mg, 95%). Electrospray ionization analysis in the positive ion mode revealed a single peak (t_R = 1.8 min) with a molecular ion ($M + H^+$) at *m/z* 343. ^{1}H NMR (DMSO-d_6): δ 8.63 (d, 1 H, ArH), 8.23 (d, 1 H, ArH), 3.93 (d, 2 H, CH_2), 2.98 (t, 2 H, CH_2), 2.46 (m, 1 H, CH), 1.89 (d, 2 H, CH_2), 1.61 (q, 2 H, CH_2).

Metabolism of Tpo Receptor Agonists 1, 4, and 5 in Human Liver Microsomes and Cryopreserved Human Hepatocytes. Incubations of human liver microsomes were carried out at 37 °C for 60 min in a shaking water bath. The incubation volume was 1 mL and consisted of 0.1 M potassium phosphate buffer (pH 7.4) containing human liver microsomes ([P450] = 0.5 μM), NADPH (1.2 mM), and test compound (50 μM). The reaction mixture was prewarmed at 37 °C for 2 min before the addition of NADPH; incubations that lacked NADPH served as negative controls. Reactions were terminated by the addition of ice-cold acetonitrile (1 mL). The solutions were centrifuged (3000*g*, 15 min), and the supernatants were dried under a steady nitrogen stream. The residue was reconstituted with mobile phase and analyzed for metabolite formation using liquid chromatography–tandem mass spectrometry (LC–MS/MS). Cryopreserved human hepatocytes (from a pool of one female and two male livers) were thawed and suspended (2 × 10^6 viable cells/mL) in Williams' E medium supplemented with 24 mM $NaHCO_3$. Test compound (50 μM) in methanol was

incubated with hepatocytes at 37 °C for 4 h with gentle agitation. A 95:5 O_2/CO_2 gas mixture maintained at 2.5 kPa for ~5 s was passed through this mixture every hour of the incubation. Flasks were corked immediately after gassing. Reactions were stopped by the addition of 2 volumes of cold acetonitrile. Following centrifugation (3500*g*, 15 min), the supernatant was dried under a steady stream of nitrogen, and the residue was reconstituted in mobile phase and examined for metabolite formation using LC–MS/MS. Qualitative metabolite formation was assessed on a Sciex API 3000 LC–MS/MS triple-quadrupole mass spectrometer in-line with a Shimadzu LC-20AD HPLC system. An autosampler was programmed to inject 20 μL of the sample onto a Synergi Polar PR 4 μm, 4.6 × 150 mm column using a binary gradient consisting of a mixture of 95% water, 5% acetonitrile, and 0.1% formic acid (solvent A) and 95% acetonitrile, 5% water, and 0.1% formic acid (solvent B) at a flow rate of 0.8 mL/min. The LC gradient was programmed as follows: the solvent A/solvent B ratio (v/v) was held at 90:10 for 0.2 min, then adjusted from 90:10 to 10:90 over 8.5 min, and finally adjusted from 10:90 back to 90:10 over 0.5 min. The column was re-equilibrated for 3 min prior to the next analytical run. Postcolumn flow was split such that the mobile phase was introduced into the mass spectrometer via an ion-spray interface at a rate of 300 μL/min. Ionization was conducted in the positive ion mode at an ion-spray interface temperature of 400 °C, using nitrogen as the nebulizing and heating gas. The ion-spray voltage was 4.5 kV, and the orifice voltage was optimized at 40 eV. Initial Q1 scans were performed between *m*/*z* 50 and 800. Metabolites were identified by comparing $t = 0$ samples with samples at $t =$ 60 min (for microsomes) or 240 min (for hepatocytes), and structural information was generated from collision-induced dissociation (CID) spectra of the corresponding protonated molecular ions and/or comparison to spectra of synthetic standards.

Hydrolytic Stability of Tpo Receptor Agonists 1, 4, and 5 in Human Plasma. Fresh human plasma was obtained by venipuncture of a healthy adult volunteer. Blood samples were collected in heparin-coated tubes, and plasma was prepared by centrifugation. Blood products were kept on ice until they were used (<1 h postcollection). Test compound (final concentration 20 μM) in methanol was incubated with fresh human plasma (0.5 mL) at 37 °C in a shaking water bath. Periodically (0–60 min), aliquots (75 μL) of the reaction mixture were added to acetonitrile (200 μL) containing a proprietary internal standard (MW = 392, 5 μg/mL) and were analyzed for the appearance of 2-amino-4-arylthiazole. Incubations were conducted in duplicate.

Reactive Metabolite Characterization in Human Liver Microsomes. Human liver microsomes ([P450] = 0.3 μM) containing **2**, **6**, **7**, or 4-phenyl-1*H*-imidazol-2-amine (100 μM each), GSH (1 mM), and an NADPH-generating system (0.54 mM $NADP^+$, 11.5 mM $MgCl_2$, 6.2 mM DL-isocitric acid, and 0.5 unit/mL isocitric acid dehydrogenase) in 100 mM potassium phosphate buffer (pH 7.4) were incubated for 60 min at 37 °C. The final incubation volume was 250 μL. Samples without either the NADPH-generating system or test compound were used as negative controls. The reactions were quenched by the addition of acetonitrile (375 μL), and the reaction mixtures were centrifuged (3500*g*, 15 min). Thiol conjugates were extracted from each sample using a Waters Oasis HLB 96-well μElution solid-phase extraction (SPE) plate. A 384-channel Personal-150 pipettor fitted with a 96-channel head (Apricot Designs, Inc., Monrovia, CA) was used during SPE extraction to facilitate solvent transfer. The SPE plate was conditioned by passing methanol (200 μL) followed by water (200 μL) through each of the SPE cartridges. To initiate solvent flow through the absorbent, vacuum was applied to the receiving side of the SPE plate using a 96-well extraction manifold (Tomtec, Inc., Hamden, CT). Samples were added to the 96-well plate and washed with water (200 μL). Analyte was desorbed using 40:60 (v/v) acetonitrile/2-propanol (100 μL). The desorption solvent was collected in a 96-well polypropylene plate. Solvent was evaporated using a 96-channel Evaporex EVX-192 evaporator (Apricot Designs) utilizing nitrogen as the drying gas. Samples were reconstituted with 5:95:0.05 (v/v) acetonitrile/water/formic acid–ammonium formate buffer (pH 3.4) (50 μL) prior to LC–MS/MS analysis. The LC–MS/MS system used to separate the GSH conjugates consisted of an Agilent 1100 pump, autosampler, and UV detector (Agilent Technologies, Palo Alto, CA) interfaced to a Finnigan LCQ Deca XP Plus (Thermo Electron Corp., San Jose, CA). Conjugates were separated via gradient HPLC using a Supelco C18 reversed-phase 5 μm, 150 × 2.1 mm column. The gradient consisted of a 5 min isocratic hold at 95:5 (v/v) 0.1% formic acid/acetonitrile followed by a linear gradient to 10:90 (v/v) 0.1% formic acid/acetonitrile over 25 min. In all cases, the flow rate was 0.4 mL/min. Postcolumn flow was split such that the mobile phase was introduced into the mass spectrometer via an electrospray interface at a rate of 50 μL/min. The remaining flow was diverted to the photodiode array detector to provide simultaneous UV detection (λ = 240–260 nm) and a total ion chromatogram. The capillary temperature was 250 °C, and CID analyses were performed using a collision energy of 30 eV. Sulfhydryl conjugates of **2** were identified in the full-scan mode (from *m*/*z* 100 to 850) by comparing $t = 0$ samples with $t = 60$ min samples (with or without cofactor or GSH), and structural information was generated from the CID spectra of the corresponding protonated molecular ions.

Reactive Metabolite Characterization in Horseradish Peroxidase. Horseradish peroxidase incubations (total volume 1 mL) were carried out at 37 °C and contained **2** (100 μM), desferoxamine (10 μM), peroxidase (3 units/mL), and GSH (1 mM) in 100 mM phosphate buffer (pH 7.0). In order to assess the role of peroxidase in the catalysis, incubations were also conducted in the presence of ascorbic acid and/or sodium azide (1 mM). The reaction was initiated by addition of H_2O_2 (500 μM), and after 60 min, the reactions were treated with catalase (300 units). The mixture was incubated for an additional 3 min, and the reaction was terminated by addition of acetonitrile (1 mL). The precipitated proteins were vortexed and centrifuged, and the resulting supernatant was used for all subsequent mass spectral analyses. Incubations that lacked peroxidase or H_2O_2 served as negative controls.

Biosynthesis and NMR Analysis of the GSH Conjugate 9. Compound **9**, the major GSH adduct of **2**, was biosynthesized via a scale-up of the NADPH-supplemented human liver microsome incubations (1 h at 37 °C) of **2** in a total of twelve 16 × 100 mm borosilicate glass tubes (2 mL incubation per tube). Cold acetonitrile (4 mL) was added to each tube, and samples were centrifuged at 1600*g* for 15 min. The supernatants were pooled, transferred to clean 20 × 150 mm borosilicate glass tubes, and evaporated to dryness in a Turbo-Vap LV under a stream of nitrogen. The residues were reconstituted in 2 mL of 0.1% acetic acid and applied to a 200 mg preconditioned SPE cartridge (Bond Elut C-18). The cartridge was washed with 3 mL of 0.1% acetic acid and eluted with successive 3 mL volumes of 95:5, 90:10, 80:20, 70:30, 60:40, 50:50, 40:60, 30:70, 20:80, and 10:90 (v/v) 0.1% acetic acid/acetonitrile. Aliquots of SPE eluate were analyzed by full-scan LC–MS/MS to determine the fraction(s) in which **9** was concentrated. The SPE fraction determined to contain the greatest amount of **9** was evaporated to dryness in a Turbo-Vap LV under a stream of nitrogen and reconstituted in mobile phase. Aliquots were injected into the analytical HPLC system described above and eluted using either a gradient or an isocratic method designed for the conjugate. The flow from the analytical column was split between a collection vessel (95%) and the mass spectrometer (5%). Isolates of **9** were collected using mass-directed fractionation, evaporated to dryness in a SpeedVac SPD 1010 centrifuge evaporator, and analyzed by NMR.

^{1}H NMR spectra were recorded on a Bruker Avance 600 MHz NMR spectrometer (Bruker BioSpin Corp., Billerica, MA) controlled by XWIN-NMR version 3.5 and equipped with a 5 mm BBI cryoprobe. Spectra were recorded using a sweep width of 5800 Hz and a total recycle time of 3 s. The resulting time-averaged free induction decays were transformed using an exponential line broadening of 0.3 Hz to enhance the signal-to-noise ratio. Samples were dissolved in 0.16 mL of "100%" methanol-d_4 (Cambridge Isotope Laboratories, Andover, MA) and placed in a 3 mm NMR tube. Spectra were referenced using residual methanol-d_4 (^{1}H δ

3.31 relative to TMS). Chemical shift predictions were calculated using ACD software (Advanced Chemistry Development, Toronto, ON).

Pharmacokinetic Studies. The Pfizer Institutional Animal Care and Use Committee approved all procedures. Sodium salts of Tpo receptor agonists **1**, **4**, and **5** were administered to fasted male Sprague-Dawley rats (200–250 g, $N = 3$ per route of administration). Compounds were administered intravenously via the jugular vein at 2 mg/kg and orally at 5 mg/kg. For all iv studies, dosing solutions were prepared in 90:10 PEG/DMSO, whereas for po studies, compounds were administered in 0.5% methylcellulose. Blood samples were collected in heparin-coated tubes via the jugular vein in series at appropriate time intervals and centrifuged to obtain plasma. Plasma samples were kept frozen until analysis. Aliquots (100 μL) of the plasma samples were treated with acetonitrile (200 μL) containing a proprietary internal standard (MW = 392, 5 μg/mL), and the samples were centrifuged at 2500*g* for 5 min prior to LC–MS/MS analysis.

Pharmacokinetic Analysis. Plasma concentration–time profiles were analyzed using the well-established noncompartmental method in WinNonLin version 2.1 (Pharsight, Mountain View, CA). The maximum plasma concentration (C_{max}) observed after po dosing and the time (t_{max}) at which it was observed were determined directly from the individual plasma concentration–time profiles. Plasma clearance (CL_p) was calculated as the iv dose divided by the area under the plasma concentration–time curve from zero to infinity ($AUC_{0-\infty}$), which was found using the linear trapezoid rule. The terminal slope of the ln(concentration) versus time plot was calculated by linear least-squares regression, and the half-life was calculated as 0.693 divided by the absolute value of this slope. The steady-state volume of distribution (V_{ss}) was determined using the noncompartmental method published by Benet and Galeazzi (*30*). The relative bioavailability (F) of po doses was calculated using the equation $F = (AUC_{0-\infty}{}^{po}/AUC_{0-\infty}{}^{iv})(dose^{iv}/dose^{po})$.

LC–MS/MS Methodology for Analysis of Tpo Receptor Agonists 1, 4, and 5. Analyte concentrations in plasma were monitored on a Sciex API 3000 LC–MS/MS triple-quadrupole mass spectrometer. Analytes were chromatographically separated using a Shimadzu LC-20 AD HPLC system. An autosampler was programmed to inject 20 μL on a Synergi Polar RP 2 μm, 30 × 2.0 mm column using a mobile phase consisting of 95:5 water/acetonitrile containing 0.1% formic acid (solvent A) and 95:5 acetonitrile/water (solvent B). The LC conditions were programmed as follows: 10% acetonitrile for 0.5 min, increasing to 90% over the next 1.8 min and then decreasing back to 10% (i.e., the original condition) over the final 3 min, at a flow rate of 0.5 mL/min. Ionization was conducted in the positive ion mode at an ion-spray interface temperature of 400 °C, using nitrogen as the nebulizing and heating gas. The ion-spray voltage was 5.0 kV, and the orifice voltage was optimized at 30 eV. Tpo receptor agonists **1**, **4**, and **5** and an internal standard were analyzed in the multiple-reaction monitoring (MRM) mode using the transitions *m/z* 529 → 267, *m/z* 547 → 267, *m/z* 530 → 267, and *m/z* 393 → 250, respectively. Calibration curves were prepared by plotting the appropriate peak-area ratios (analyte/internal standard) against the concentrations of analyte in plasma using 1/*x* weighting. The concentrations of the analytes in the plasma samples were determined by interpolation from the standard curve. The dynamic range of the assay was 2.5–10000 ng/mL.

Results

Metabolism of Tpo Receptor Agonists in Human Liver Microsomes and Hepatocytes. The susceptibility of Tpo receptor agonists toward amidase-catalyzed hydrolysis was investigated in human liver microsomes and cryopreserved human hepatocytes. LC–MS/MS analysis of incubates containing **1**, **4**, or **5** (50 μM) revealed the presence of several metabolites as well as unreacted parent compound. A common metabolite detected in incubations of all three compounds appeared at $t_R \sim 9.7$ min and possessed a molecular ion (MH^+) of 285 Da. The t_R and mass spectrum of this metabolite (Figure 1) were identical to those of the authentic standard of **3**; the metabolite appeared to be derived from hydrolytic cleavage of the parent compounds. Besides **3**, the formation of the 2-amino-4-aryl heterocyclic metabolites **2**, **6**, and **7** was also discernible in microsome/hepatocyte incubations of **1**, **4**, and **5**, respectively. Metabolites **2**, **6**, and **7** were unambiguously identified by comparing t_R and mass spectral characteristics with those of their authentic standards. In the case of human liver microsome incubations, the hydrolyses of **1**, **4**, and **5** were NADPH-independent, suggesting that amide bond cleavage was mediated by proteolytic enzymes (esterases/amidases).

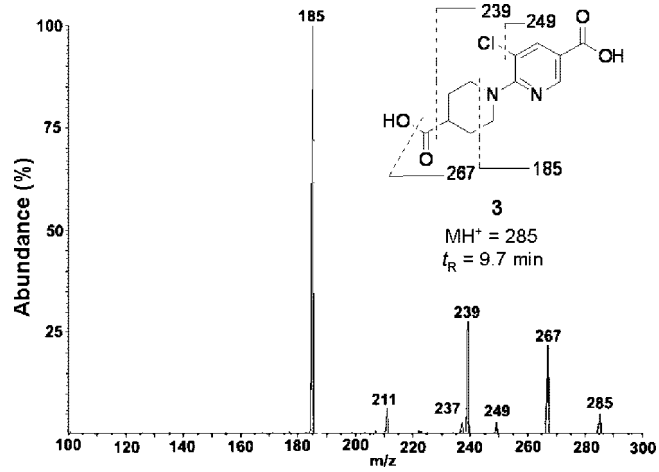

Figure 1. Product ion spectrum obtained by CID of the MH^+ ion (*m/z* 285) of the metabolite 6-(4-carboxypiperidin-1-yl)-5-chloronicotinic acid **3** observed in cryopreserved human hepatocyte incubations containing Tpo receptor agonists **1**, **4**, and **5**. The t_R and mass spectral characteristics of **3** were identical to those of an authentic standard. The proposed origins of the characteristic ions are as indicated.

In addition to the products of hydrolysis, glucuronidation of the carboxylic acid groups in **1**, **4**, and **5** was also detected in hepatocyte incubations. Metabolites at $t_R \sim 8.77$, 14.6, and 13.9 min possessed molecular ions of 705, 723, and 706 Da, respectively, consistent with direct glucuronidation of the respective parent compounds **1**, **4**, and **5**; these metabolites were tentatively assigned as the corresponding acyl glucuronides derived from phase-II conjugation of the carboxylic acid group (Figure 2). The availability of synthetic standards of the thiazole ring scission products of **1** allowed us to specifically track the formation of these intermediates in human liver microsome and hepatocyte incubations. It is noteworthy to point out that 1-(3-chloro-5-(thioureidocarbonyl)pyridin-2-yl)piperidine-4-carboxylic acid and 2-(4-fluoro-3-(trifluoromethyl)phenyl)-2-oxoacetaldehyde (and/or its corresponding carboxylic acid derivative), putative products of thiazole ring scission in **1**, were not observed upon LC–MS/MS analysis of human liver microsome or human hepatocyte incubations of **1**.

Hydrolytic Stability of Tpo Receptor Agonists in Human Plasma. Hydrolytic stability of Tpo receptor agonists was further assessed following incubation of test compound (20 μM) in fresh human plasma at 37 °C. As shown in Figure 3, periodic LC–MS/MS analysis of aliquots of incubations of **1**, **4**, and **5** in human plasma revealed the formation of the 2-amino-4-aryl heterocyclic metabolites **2**, **6**, and **7**, respectively. Interestingly, the extent of hydrolysis of **4** and **5** was less than that of **1**.

Characterization of GSH Adducts. LC–MS/MS analysis of NADPH-supplemented human liver microsome incubations containing synthetic **2** and GSH led to the detection of the two

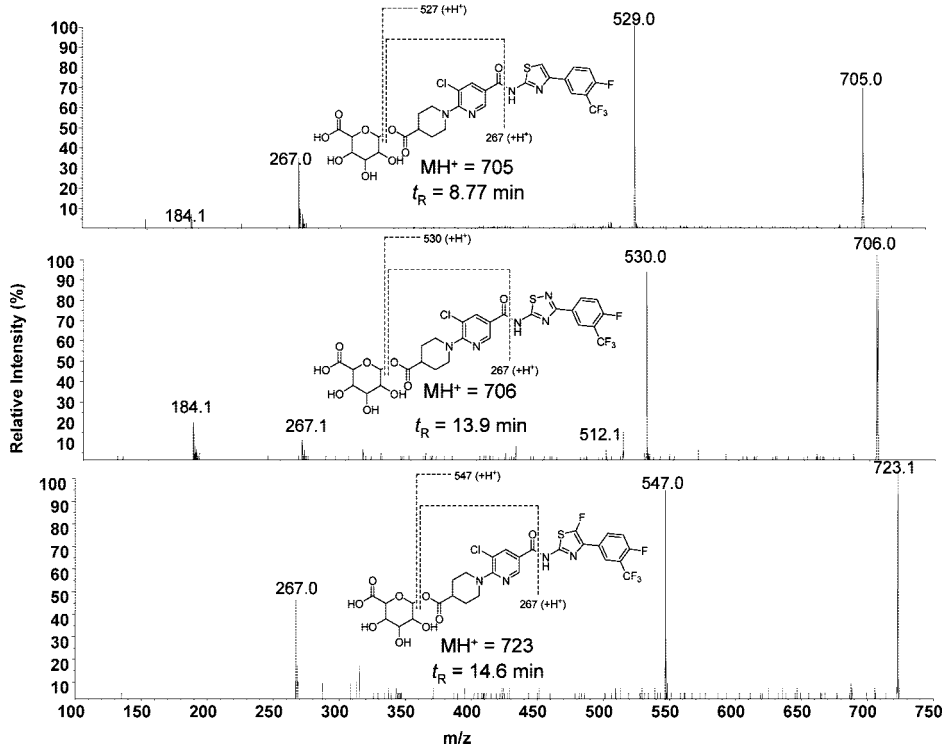

Figure 2. Product ion spectra obtained by CID of the MH^+ ions of the acyl glucuronide metabolites observed in cryopreserved human hepatocyte incubations containing Tpo receptor agonists **1**, **5**, and **4**. The proposed origins of the characteristic ions are as indicated.

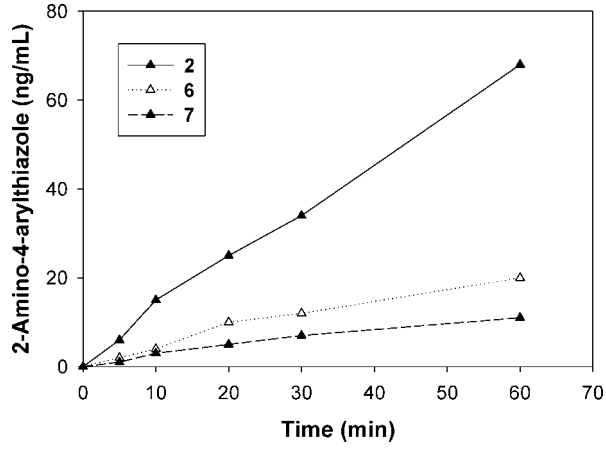

Figure 3. Liberation of 2-amino-4-arylthiazole metabolites **2**, **6**, and **7** following incubation of Tpo receptor agonists **1**, **4**, and **5**, respectively, in fresh human plasma at 37 °C. Data depicted are means of two separate determinations.

thiol conjugates **8** (t_R = 14.61 min, Figure 4A) and **9** (t_R = 15.15 min, Figure 4B) with ions at *m/z* 568 and 584, respectively. The molecular weights of **8** and **9** were consistent with the addition of one molecule of GSH to **2** and a monohydroxylated metabolite of **2**, respectively.

The CID spectrum of GSH conjugate **8** (Figure 5) contained product ions at *m/z* 493 and 439, resulting from the prototypical neutral losses of glycine (75 Da) and pyroglutamate (129 Da), respectively (*31*). The fragment ion at *m/z* 293 (Figure 5) was assigned as the product of a cleavage adjacent to the cysteinyl thioether moiety with charge retention on the 2-amino-4-arylthiazole residue. Furthermore, the occurrence of this fragment ion is consistent with the presence of an aromatic thioether motif in **8** (*31*). The presence of the fragment ion at *m/z* 177, which is also present in the mass spectrum of **2** (Figure 6) and corresponds to a tropylium cation, suggested that the site of attachment of GSH within **8** is not on the phenyl ring. On the basis of these findings, a proposed structure of **8** consistent with its fragmentation pattern is shown in Figure 5.

The product-ion spectrum of the major GSH conjugate **9** (MH^+ = 584) is depicted in Figure 7. The presence of the fragment ion at *m/z* 455 was consistent with the loss of the pyroglutamate moiety in **9**. Likewise, the fragment ion at *m/z* 491 is consistent with the losses of glycine and fluorine components. The fragment ion at *m/z* 310 occurred due to cleavage adjacent to the cysteinyl thioether moiety, again consistent with the presence of an aromatic thioether motif in **9** (*31*). Additional structural details of **9** were obtained by NMR spectroscopy. Figure 8A depicts the aromatic region of the NMR spectrum of **9**. For comparison, the aromatic region for 2-amino-4-arylthiazole **2** is shown in Figure 8B. The site of attachment of the glutathionyl moiety was determined to be the C5 position of the thiazole ring, since the C5 proton was conspicuously absent in the NMR spectrum of **9**. Furthermore, the presence of all aromatic protons in the NMR spectrum of **9** indicates that oxygenation does not occur on the phenyl ring but on a heteroatom in the 2-aminothiazole ring in **9**. The site of oxygenation was further probed by the use of titanium trichloride reduction methodology (*32*) and via reactive metabolite trapping studies on 4-phenyl-1*H*-imidazol-2-amine, a 2-amino-4-arylthiazole analogue in which the sulfur atom is replaced by the NH motif and therefore should not undergo the S-oxidation process. Under reaction conditions that led to a facile reduction of the *N*-oxide motif in a positive control, minoxidil (*33*), **9** failed to undergo reduction (as detected by monitoring via LC–MS/MS for loss of 16 Da) after reaction with titanium trichloride for 1 h. This observation suggests that oxygen incorporation did not occur on the thiazole-ring nitrogen or on the 2-amino group in **9**, since the corresponding oxidation product in each case (i.e., the *N*-oxide or the hydroxylamine, respectively) is known to undergo reduction under such conditions (*32, 34*). Furthermore, this result is consistent with the fact that *S*-oxides are resistant to titanium trichloride reduction (*32*). LC–MS/MS

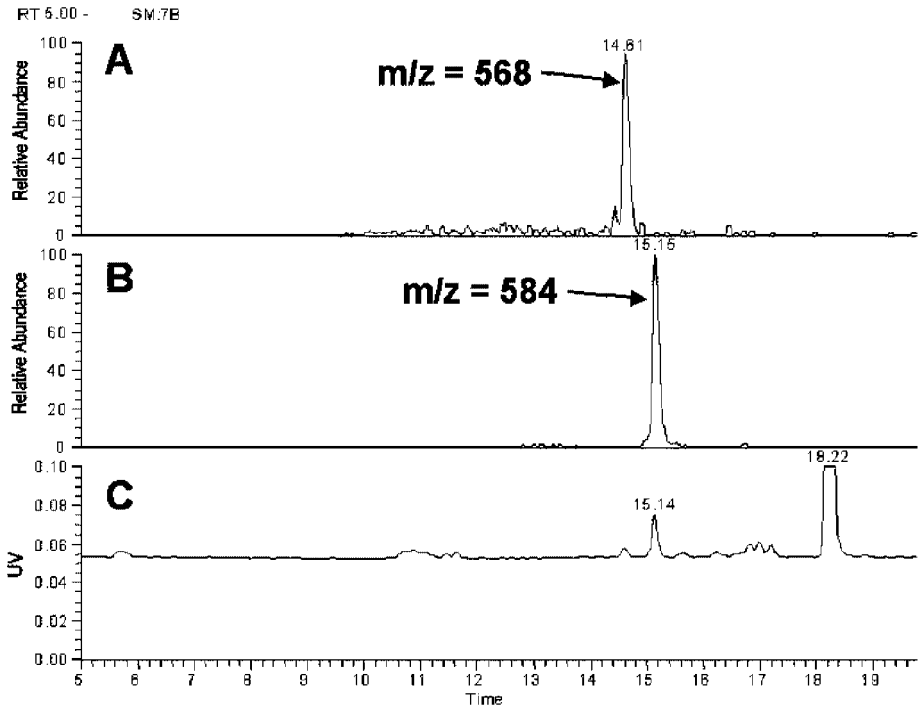

Figure 4. Extracted-ion [(A) *m*/*z* 568 and (B) *m*/*z* 584] and (C) UV ($\lambda = 254$ nm) chromatograms of an NADPH- and GSH-supplemented human liver microsome incubation containing 4-(4-fluoro-3-(trifluoromethyl)phenyl)thiazol-2-amine **2**.

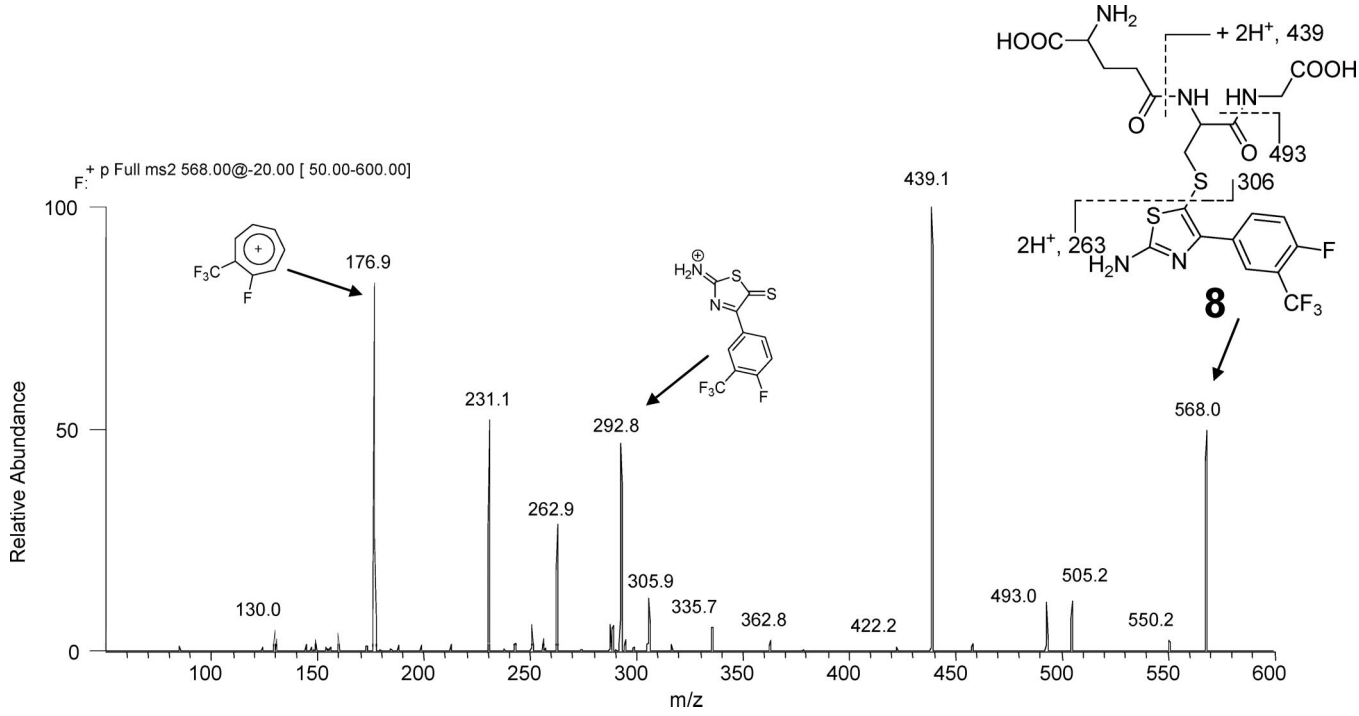

Figure 5. Product-ion spectrum obtained by CID of the MH^+ ion (*m*/*z* 568) of the GSH conjugate **8** derived from the addition of GSH to 4-(4-fluoro-3-(trifluoromethyl)phenyl)thiazol-2-amine **2** in NADPH- and GSH-supplemented human liver microsomes. The proposed origins of the characteristic ions are as indicated.

analysis of NADPH-supplemented human liver microsome incubations containing 4-phenyl-1*H*-imidazol-2-amine and GSH led to the detection of a single thiol conjugate ($t_R = 10.31$ min, Figure 9A,B) with a molecular ion MH^+ at *m*/*z* 465. The molecular weight of this conjugate was consistent with the addition of one molecule of GSH to 4-phenyl-1*H*-imidazol-2-amine. No GSH conjugate corresponding to the addition of GSH to a monohydroxylated metabolite of 4-phenyl-1*H*-imidazol-2-amine was discernible in these incubations. As a result of these analyses, the regiochemistry of oxygenation was assigned to the sulfur atom on the thiazole ring in **9**, as shown in Figures 7 and 8.

LC–MS/MS analysis of NADPH- and GSH-supplemented human liver microsome incubations of 2-amino-4-aryl-5-fluorothiazole **6** and 2-amino-4-arylthiadiazole **7**, the metabolites of Tpo receptor agonists **4** and **5**, respectively, did not indicate the formation of GSH conjugates of **6** and **7** upon monitoring both for the constant neutral loss of 129 Da and for the presence

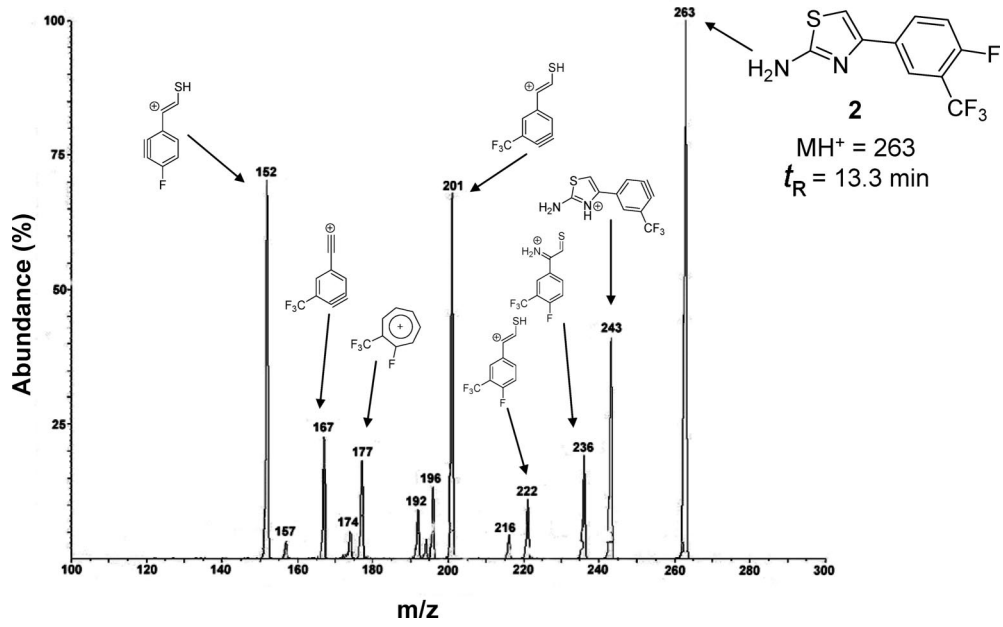

Figure 6. Product-ion spectrum obtained by CID of the MH^+ ion (*m/z* 263) of the metabolite 4-(4-fluoro-3-(trifluoromethyl)phenyl)thiazol-2-amine **2** observed in cryopreserved human hepatocyte incubations containing Tpo receptor agonist **1**. The t_R and mass spectral attributes of this metabolite were identical to those of the corresponding authentic standard. The proposed origins of the characteristic ions are as indicated.

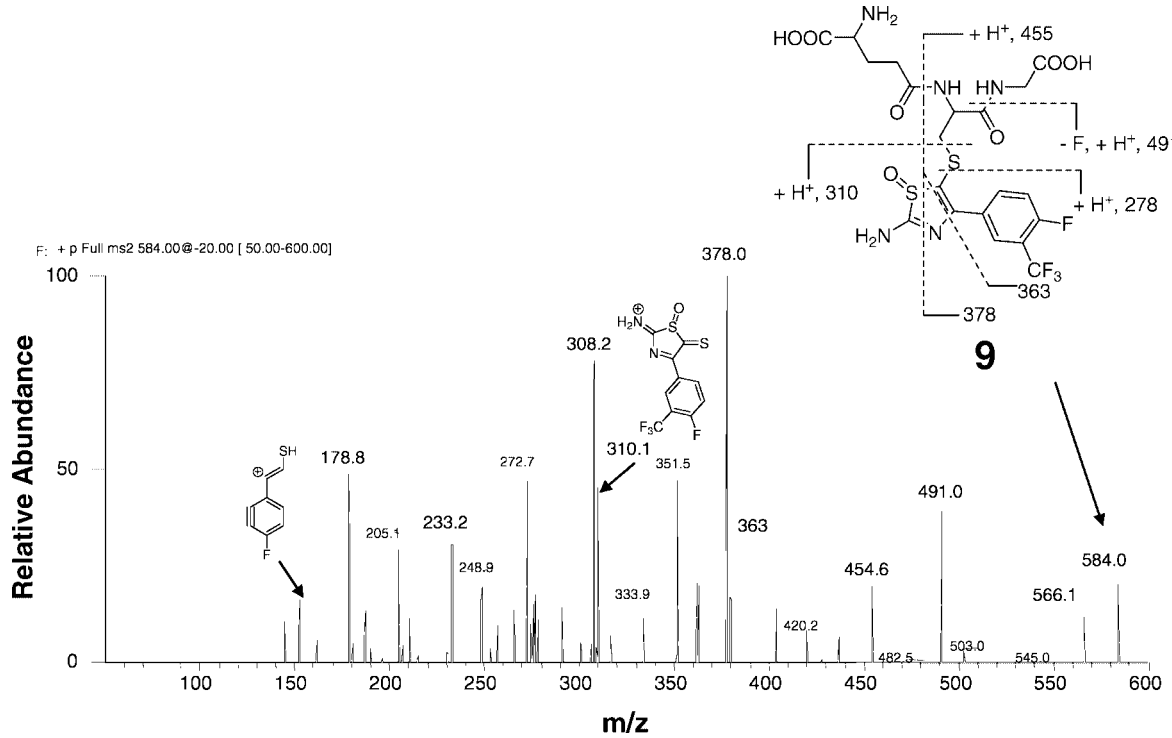

Figure 7. Product-ion spectrum obtained by CID of the MH^+ ion (*m/z* 584) of GSH conjugate **9** derived from the addition of GSH to a monohydroxylated metabolite of 4-(4-fluoro-3-(trifluoromethyl)phenyl)thiazol-2-amine **2** in NADPH- and GSH-supplemented human liver microsomes. The proposed origins of the characteristic ions are as indicated.

of multiple reactions [loss of the pyroglutamate moiety from the anticipated molecular ion(s) of the GSH conjugates] using the MRM mode.

Bioactivation Studies in Horseradish Peroxidase. 2-Amino-4-arylthiazole **2** readily formed GSH adduct **8** ($MH^+ = 568$) upon incubation with horseradish peroxidase. This adduct had an HPLC retention time and product-ion spectrum identical to those obtained from the GSH conjugate **8** formed in human liver microsomes. The formation of **8** was peroxidase- and H_2O_2-dependent. Addition of ascorbic acid and sodium azide (final concentrations 1 mM) as inhibitors of peroxidases resulted in inhibition of GSH conjugate formation (data not shown). Furthermore, the addition of desferoxamine mesylate, an iron chelator, to the incubation mixtures did not inhibit bioactivation, suggesting that the reaction was enzyme-mediated. Comparison of the peak areas of **8** formed in liver microsomes and horseradish peroxidase revealed that the yield was ~64-fold greater in the peroxidase incubation (peak areas of **8** in liver microsomes and horseradish peroxidase were 2926 ± 453 and 187 796 ± 54 479, respectively). The formation of GSH

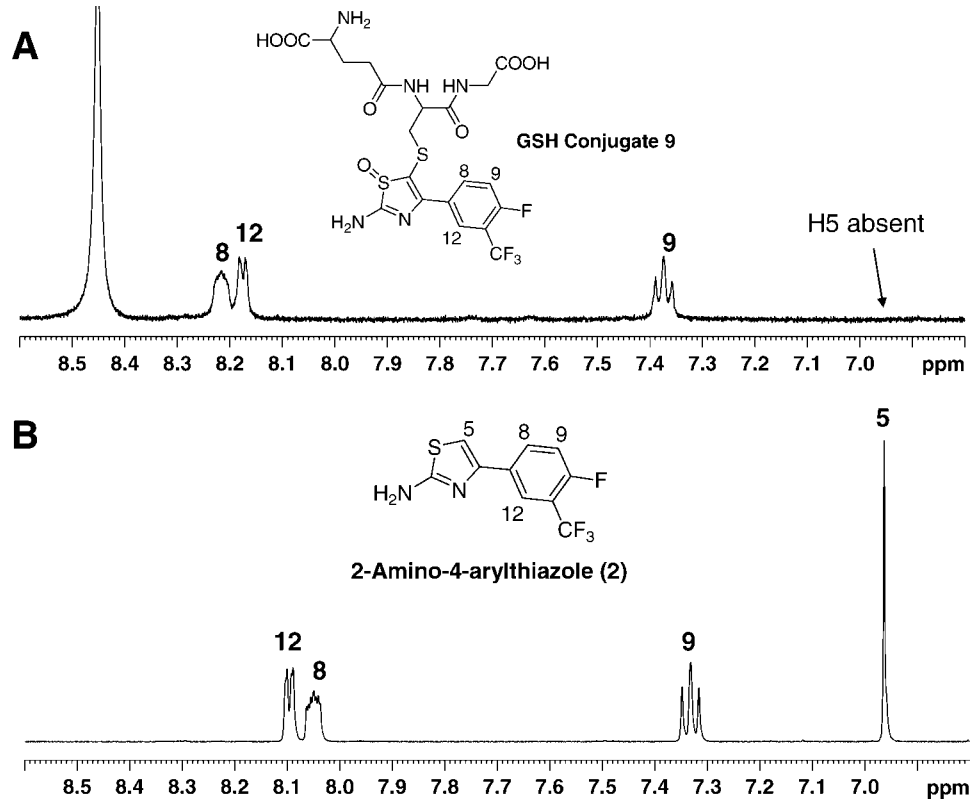

Figure 8. (A) Aromatic region of the ^{1}H NMR spectrum of the GSH conjugate **9** derived from the addition of GSH to a monohydroxylated metabolite of 4-(4-fluoro-3-(trifluoromethyl)phenyl)thiazol-2-amine **2** in NADPH- and GSH-supplemented human liver microsomes. (B) The aromatic region of the ^{1}H NMR spectrum of **2**, shown for the purpose of comparison to (A).

conjugate **9** was not discernible in peroxidase incubations. No GSH conjugates were observed upon incubation of horseradish peroxidase/H_2O_2 with 2-amino-4-aryl-5-fluorothiazole **6** or 2-amino-4-arylthiadiazole **7**.

Pharmacokinetic Analysis of 1, 4, and 5 in Sprague-Dawley Rats. Table 1 summarizes the values (mean ± SD) of the pharmacokinetic parameters for **1**, **4**, and **5** after iv and po administration of individual compounds at 2 and 5 mg/kg, respectively. Plasma concentrations after iv administration of Tpo receptor agonist **1** declined steadily, with a terminal half-life of 1.34 ± 0.25 h. CL_p and V_{ss} averaged 6.89 ± 0.05 mL min^{-1} kg^{-1} and 0.83 ± 0.09 L/kg, respectively. The value of C_{max} observed after po administration of **1** was 2.05 ± 0.25 μg/mL and occurred at a time $t_{max} = 0.75 \pm 0.35$ h after dosing; the corresponding $AUC_{0-\infty}$ was 8.1 ± 1.3 μg h mL^{-1}. Overall, **1** demonstrated good oral bioavailability in these animals (F = 66.8 ± 10.9%). The iv pharmacokinetics of **4** and **5** were comparable to those of **1**. For instance, both **4** and **5** exhibited low values of both CL_p (2.79 ± 0.74 and 1.49 ± 0.13 mL/min/kg, respectively) and V_{ss} (0.34 ± 0.05 and 0.22 ± 0.05 L/kg, respectively), resulting in terminal half-lives of 1.67 ± 0.17 and 1.09 ± 0.06 h, respectively. Likewise, as displayed in Table 1, the po pharmacokinetic attributes of **4** and **5** were similar to those of **1**, resulting in F values of 73.0 ± 1.0 and 73.5 ± 2.5%, respectively.

Tpo Receptor Agonist Assay. The murine hematopoietic IL3-dependent cell line BaF3 transfected with the human Tpo receptor and the STAT1/3-responsive β-lactamase reporter gene was used to assess Tpo receptor agonism. This reporter is based upon Aurora technology (*35*) and measures the induction of β-lactamase enzymatic activity in response to stimulation of the Tpo receptor. In this assay, compound **1** demonstrated an EC_{50} of 87 nM, while compounds **4** and **5** exhibited EC_{50} values of 88 nM and 500 nM, respectively.

Discussion

From a drug metabolism standpoint, the otherwise attractive pharmacological and pharmacokinetic attributes of **1** were offset by the presence of the 2-carboxamido-4-arylthiazole motif as part of the core structure in **1**. Fairly strong evidence linking thiazole ring bioactivation to subsequent toxicological response in preclinical species and/or humans has been presented for numerous thiazole-containing xenobiotics, including drugs (*16*). A dramatic example wherein elimination of the bioactivation liability due to thiazole ring opening has also resulted in the elimination of hepatotoxicity in the successor agent is provided by the 2-carboxamidothiazole-based nonsteroidal anti-inflammatory drugs (NSAIDs) sudoxicam and meloxicam. The clinical hepatotoxic effects of sudoxicam have been circumstantially linked to the bioactivation of its thiazole ring to reactive thioureido and thiourea metabolites (*36, 37*). In contrast, meloxicam does not appear to possess the hepatotoxic liability associated with its predecessor. Although a methyl group at the thiazole C5 position in meloxicam is the only structural difference between the two NSAIDs, this change dramatically alters the metabolic profile such that oxidation of the C5 methyl group to a carboxylic acid derivative represents the principal metabolic fate of meloxicam in humans and no thiazole ring opening is observed (*38*). In the present study, safety concerns regarding metabolites generated from the thiazole ring-opening pathway were alleviated by virtue of the fact that LC–MS/MS analysis of human liver microsome and/or hepatocyte incubations of **1** did not indicate the formation of the putative thioureido and glyoxal metabolites that could result from thiazole ring scission. This finding appears to be consistent with previous structure–metabolism relationship studies wherein the presence of C4 and/or C5 substituents on the thiazole ring has been shown to sterically hinder P450-mediated epoxidation and thus prevent thiazole ring cleavage (*20, 21*).

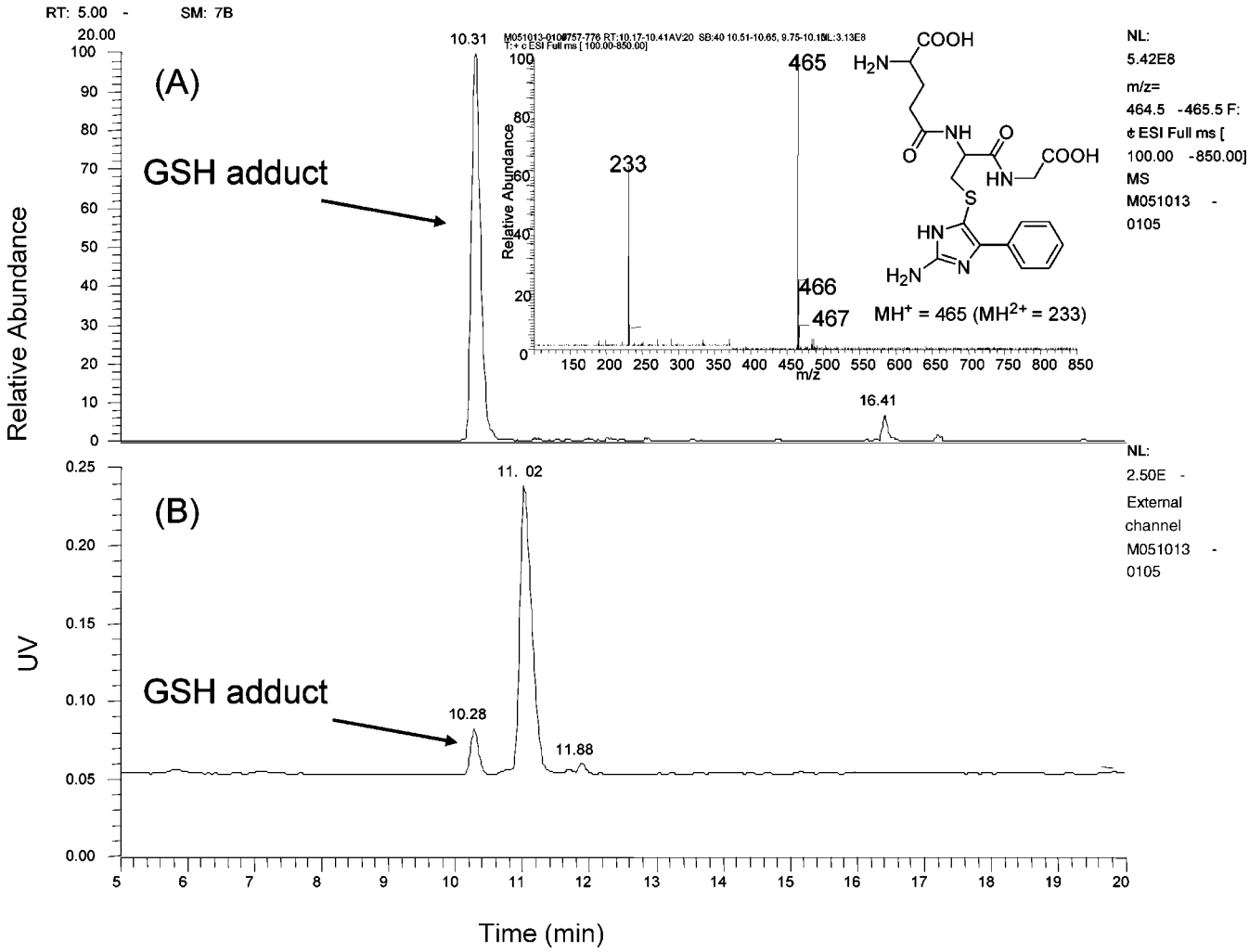

Figure 9. (A) Extracted-ion (*m*/*z* 465) and (B) UV (λ = 254 nm) chromatograms of a NADPH- and GSH-supplemented human liver microsome incubation containing 4-phenyl-1*H*-imidazol-2-amine.

Table 1. Pharmacokinetic Parameters of Tpo Agonists 1, 4, and 5 in Sprague-Dawley Rats[a]

compound	dose (mg/kg)	route	C_{max} (μg/mL)	t_{max} (h)	$t_{1/2}$ (h)	CL_p (mL min^{-1} kg^{-1})	V_{ss} (L/kg)	$AUC_{0-\infty}$ (μg h mL^{-1})	F (%)
1	1	iv[b]	NA	NA	1.34 ± 0.25	6.89 ± 0.05	0.83 ± 0.09	4.85 ± 0.03	NA
	5	po[c]	2.05 ± 0.25	0.75 ± 0.35	0.96 ± 0.049	NA	NA	8.10 ± 1.32	66.8 ± 11
4	1	iv[b]	NA	NA	1.67 ± 0.17	2.79 ± 0.74	0.34 ± 0.05	12.4 ± 3.30	NA
	5	po[c]	5.82 ± 0.64	0.63 ± 0.53	1.98 ± 0.70	NA	NA	22.6 ± 0.30	73.0 ± 1.0
5	1	iv[b]	NA	NA	1.09 ± 0.06	1.49 ± 0.13	0.22 ± 0.05	22.8 ± 1.96	NA
	5	po[c]	10.1 ± 0.71	0.75 ± 0.35	1.72 ± 0.52	NA	NA	42.0 ± 1.46	73.5 ± 2.5

[a] All values reported as mean ± SD. NA indicates data not available. [b] Compounds were administered via iv bolus to fasted Sprague-Dawley rats (N = 3) at 2 mg/kg in 90:10 PEG/DMSO. [c] Compounds were administered via po gavage to fasted Sprague-Dawley rats (N = 3) at 5 mg/kg in 0.5% methylcellulose.

While ring scission did not occur, **1** underwent carboxylesterase-mediated amide bond hydrolysis in hepatic tissue and plasma in a manner similar to that observed with the NSAID piroxicam (*39*). Piroxicam is a close structural analogue of sudoxicam and meloxicam wherein the 2-aminothiazole motif is replaced with a 2-aminopyridine substituent. The observation that hydrolytic cleavage in **1** liberated the corresponding 2-amino-4-arylthiazole metabolite **2** was a concern, considering that analogous 2-aminothiazoles, which include ANFT, are known carcinogens and mutagens in animals and humans (*24, 25, 40*). Furthermore, evaluation of the biochemical basis for the carcinogenic/mutagenic response of ANFT and related analogues has suggested that oxidative metabolism to reactive species is a likely rate-limiting step in the ensuing toxicity (*24, 25, 41*). In addition to these liabilities, the parent 2-aminothiazole itself has been shown to inactivate heme-containing peroxidases in a manner consistent with mechanism-based inactivation (*42*). The availability of the synthetic standard of **2** allowed a thorough assessment of its bioactivation potential. Incubation of **2** in NADPH- and GSH-supplemented human liver microsomes led to the characterization of the two GSH conjugates **8** and **9** obtained via addition of the sulfhydryl nucleophile to **2** and a monohydroxylated metabolite of **2**, respectively. Mass spectral and NMR analysis strongly suggested that the site of attachment of the glutathionyl moiety was the C5 position of the thiazole ring. The proposed structure of **8** is analogous to that of the previously characterized GSH adduct derived from conjugation of the sulfhydryl nucleophile to ANFT following its bioactivation by horseradish peroxidase (*41*). The finding that GSH conjugation occurs at the C5 position of the thiazole ring also lends support to the existence of two bioactivation pathways involving the oxidation

of **2**, one to an electrophilic C5 carbocation intermediate (Scheme 1, pathway B) and the other to a radical intermediate (Scheme 1, pathway C). A mechanism employing two sequential one-electron oxidations (Scheme 1, pathway C) would also be consistent with the fact that the GSH conjugate **8** formed in liver microsomes is also generated by horseradish peroxidase, an enzyme that is known to oxidize substrates by this mechanism. A similar mechanism has been invoked for the peroxidase-catalyzed metabolism of acetaminophen and zafirlukast to reactive intermediates (*43, 44*). While the results of our reactive metabolite trapping studies on 4-phenyl-1*H*-imidazol-2-amine and the failure of **9** to undergo $TiCl_3$-mediated reduction strongly suggest that the site of oxidation in **9** is the sulfur atom, from a mechanistic point of view the pathway leading to the formation of **9** remains unclear. On the basis of the available literature concerning S-oxidation of thiazoles (*45, 46*), we speculate that **2** initially undergoes oxygenation of the thiazole sulfur to the corresponding *S*-oxide, followed by its further two-electron oxidation to a reactive species. Additional studies to address this unique oxidation pathway are currently ongoing.

Overall, given this information, it appeared reasonable to attempt to minimize or eliminate bioactivation liability in the prototype Tpo receptor agonist **1** through rationally designed small structural modifications of the thiazole ring. The C5 fluoro and thiadiazole analogues **4** and **5** were prepared under the assumption that the corresponding hydrolysis products, namely, the 2-amino heterocyclic metabolites **6** and **7**, would not succumb to the bioactivation pathways found for **2**. The absence of GSH conjugate formation in incubations of microsomes with **6** and **7** was consistent with the proposed bioactivation mechanism of **2** leading to GSH conjugates **8** and **9**. Interestingly, these subtle structural changes designed to eliminate bioactivation liability also decreased the extent of amide bond hydrolysis. Although the reason(s) for the differential rates of hydrolysis following subtle structural changes at a site distant from the amide bond cleavage remains unclear, it is noteworthy to point out that similar observations have been noted in some structure–metabolism relationship studies of amide/ester bond hydrolysis (*47*). Of great interest was the finding that the C5 fluoro analogue **4** retained the potent and selective in vitro Tpo receptor agonist properties as well as the attractive pharmacokinetic attributes of **1** found in rats and predicted in humans [given the fact that both **1** and **4** were highly protein bound (∼99%), the unbound maximal systemic exposures of the two compounds were comparable and aligned with their in vitro functional agonist activities]. This result is fairly important, since subtle structural changes devised to fix a potential liability can dramatically affect primary pharmacology and/or otherwise optimal disposition properties.

While the toxicity risk associated with the bioactivation of the 2-aminothiazole group in **1** was eliminated with **4** and **5**, the finding that both **4** and **5** generated acyl glucuronide conjugates in a fashion similar to that of **1** represented the final hurdle to compound progression from a metabolism/safety viewpoint. A causal relationship between covalent protein modification by acyl glucuronide metabolites and NSAID toxicity has been established (*48, 49*). Two pathways have been proposed to account for such covalent adduct formation: (a) protein transesterification and (b) Schiff base formation, in which condensation occurs between the aldehyde group of a rearranged acyl glucuronide and either a lysine residue or an amine group of the N terminus, leading to the formation of a glycated protein. A structural relationship between acyl glucuronide degradation to the Schiff base and covalent binding has been proposed (*50*). Acyl glucuronides of acetic acid derivatives exhibit the highest level of rearrangement and covalent binding, whereas mono-α-substituted acetic acids exhibit low to intermediate levels of acyl glucuronide rearrangement and covalent binding, implying that inherent electronic and steric properties can modulate the rates of acyl glucuronide rearrangement (*51, 52*). In this context, it is important to note the lack of acyl glucuronide migration observed with **1**, **4**, and **5**, reflected by the presence of only a single acyl glucuronide peak upon analysis by LC–MS/MS over time (data not shown). This implies that the piperidine ring, which is directly attached to the carboxylic acid functionality, must sterically hinder acyl glucuronide migration in a manner similar to that observed with α-substituted acetic acid compounds, thus mitigating the overall risk of toxicity due to acyl glucuronidation.

In summary, we have demonstrated the human liver microsomal bioactivation of a 2-amino-4-arylthiazole functionality present as part of the core structure of a novel Tpo receptor agonist. Characterization of its GSH adducts using LC–MS/MS and NMR techniques provided indirect information on the structures of electrophilic intermediates, thereby providing insight into the bioactivation mechanism. The information derived from these studies was used to direct medicinal chemistry efforts in the design of agonists that maintained the attractive primary pharmacological and pharmacokinetic attributes of the prototype compound while avoiding the safety concerns associated with its 2-aminothiazole motif. Studies are currently in progress to examine whether the bioactivation mechanism described here for 2-aminothiazoles applies generally to all 2-aminoheterocycles containing two heteroatoms.

References

(1) Kaushansky, K. (2005) The molecular mechanisms that control thrombopoiesis. *J. Clin. Invest. 115*, 3339–3347.

(2) Solberg, L. A., Jr. (2005) Biologic aspects of thrombopoietins and the development of therapeutic agents. *Curr. Hematol. Rep. 4*, 423–428.

(3) Drachman, J. G., Sabath, D. F., Fox, N. E., and Kaushansky, K. (1997) Thrombopoietin signal transduction in purified murine megakaryocytes. *Blood 89*, 483–492.

(4) Ezumi, Y., Takayama, H., and Okuma, M. (1995) Thrombopoietin, c-Mpl ligand, induces tyrosine phosphorylation of Tyk2, JAK2, and STAT3, and enhances agonists-induced aggregation in platelets in vitro. *FEBS Lett. 374*, 48–52.

(5) Rojnuckarin, P., Drachman, J. G., and Kaushansky, K. (1999) Thrombopoietin-induced activation of the mitogen-activated protein kinase (MAPK) pathway in normal megakaryocytes: role in endomitosis. *Blood 94*, 1273–1282.

(6) de Sauvage, F. J., Hass, P. E., Spencer, S. D., Malloy, B. E., Gurney, A. L., Spencer, S. A., Darbonne, W. C., Henzel, W. J., Wong, S. C., Kuang, W. J., Oles, K. J., Hultgren, B., Jr., Goeddel, D. V., and Eaton, D. L. (1994) Stimulation of megakaryocytopoiesis and thrombopoiesis by the c-Mpl ligand. *Nature 369*, 533–538.

(7) Foster, D. C., Sprecher, C. A., Grant, F. J., Kramer, J. M., Kuuper, J. L., Holly, R. D., Whitmore, T. E., Heipel, M. D., Bell, L. A., Ching, A. F. T., McGrane, V., Hart, C., O'Hara, P. J., and Lok, S. (1994) Human thrombopoietin: Gene structure, cDNA sequence, expression, and chromosomal localization. *Proc. Natl. Acad. Sci. U.S.A. 91*, 130223–130227.

(8) Kaushansky, K., Lok, S., Holly, R. D., Broudy, V. C., Lin, N., Bailey, M. C., Forstrom, J. W., Buddle, M. M., Oort, P. J., Hagen, F. S., Roth, G. J., Papayannopoulou, T., and Foster, D. C. (1994) Promotion of megakaryocyte progenitor expansion and differentiation by the c-Mpl ligand thrombopoietin. *Nature 369*, 568–571.

(9) Lok, S., Kaushansky, K., Holly, R. D., Kuijper, J. L., Lofton-Day, C. E., Oort, P. J., Grant, F. J., Heipel, M. D., Burkhead, S. K., Kramer, J. M., Bell, L. A., Sprecher, C. A., Blumberg, H., Johnson, R., Prunkard, D., Ching, A. F. T., Mathewes, S. L., Bailey, M. C., Forstrom, J. W., Buddle, M. M., Osborn, S. G., Evans, S. J., Sheppard, P. O., Presnell, S. R., O'Hara, P. J., Hagen, F. S., Roth, G. J., and Foster, D. C. (1994) Cloning and expression of murine thrombopoietin cDNA and stimulation of platelet production in vivo. *Nature 369*, 565–568.

(10) Nash, R. A., Kurzrock, R., DiPersio, J., Linker, C., Maharaj, D., Nademanee, A. P., Negrin, R., Nimer, S., Shulman, H., Ashby, M., Jones, D., Appelbaum, F. R., and Champlin, R. (2000) A phase I trial of recombinant human thrombopoietin in patients with delayed platelet

recovery after hematopoietic stem cell transplantation. *Biol. Blood Marrow Transplant. 6*, 25–34.
(11) Safonov, I. G., Heerding, D. A., Keenan, R. M., Price, A. T., Erickson-Miller, C. L., Hopson, C. B., Levin, J. L., Lord, K. A., and Tapley, P. M. (2006) New benzimidazoles as thrombopoietin receptor agonists. *Bioorg. Med. Chem. Lett. 16*, 1212–1216.
(12) Duffy, K. J., Price, A. T., Delorme, E., Dillon, S. B., Duquenne, C., Erickson-Miller, C., Giampa, L., Huang, Y., Keenan, R. M., Lamb, P., Liu, N., Miller, S. G., Rosen, J., Shaw, A. N., Smith, H., Wiggall, K. J., Zhang, L., and Luengo, J. I. (2002) Identification of a pharmacophore for thrombopoietic activity of small, non-peptidyl molecules. 2. Rational design of naphtho[1,2-d]imidazole thrombopoietin mimics. *J. Med. Chem. 45*, 3576–3578.
(13) Duffy, K. J., Darcy, M. G., Delorme, E., Dillon, S. B., Eppley, D. F., Erickson-Miller, C., Giampa, L., Hopson, C. B., Huang, Y., Keenan, R. M., Lamb, P., Leong, L., Liu, N., Miller, S. G., Price, A. T., Rosen, J., Shah, R., Shaw, T. N., Smith, H., Stark, K. C., Tian, S. S., Tyree, C., Wiggall, K. J., Zhang, L., and Luengo, J. I. (2001) Hydrazinonaphthalene and azonaphthalene thrombopoietin mimics are nonpeptidyl promoters of megakaryocytopoiesis. *J. Med. Chem. 44*, 3730–3745.
(14) Kimura, T., Kaburaki, H., Tsujino, T., Ikeda, Y., Kato, H., and Watanabe, Y. (1998) A non-peptide compound which can mimic the effect of thrombopoietin via c-Mpl. *FEBS Lett. 428*, 250–254.
(15) Munchhof, M. J., Abramov, Y. A., Antipas, A. S., Blumberg, L. C., Brissette, W. H., Brown, M. F., Casavant, J. M., Doty, J. L., Driscoll, J., Harris, T. M., Wolf-Gouveia, L. A., Jones, C. S., Li, Q., Linde, R. G., Lira, P. D., Marfat, A., McElroy, E., Mitton-Fry, M., McCurdy, S. P., Reiter, R. A., Ripp, S. L., Shavnya, A., Shepard, R. M., Smeets, M. I., Sperger, D., Thomasco, L. M., Trevena, K. A., Zhang, F., and Zhang, L. (2007) The Identification of Orally Bioavailable Thrombopoietin Agonists. *Bioorg. Med. Chem. Lett.*, in press.
(16) Kalgutkar, A. S., Gardner, I., Obach, R. S., Shaffer, C. L., Callegari, E., Henne, K. R., Mutlib, A. E., Dalvie, D. K., Lee, J. S., Nakai, Y., O'Donnell, J. P., Boer, J., and Harriman, S. P. (2005) A comprehensive listing of bioactivation pathways of organic functional groups. *Curr. Drug Metab. 6*, 161–225.
(17) Evans, D. C., Watt, A. P., Nicoll-Griffith, D. A., and Baillie, T. A. (2004) Drug-protein adducts: an industry perspective on minimizing the potential for drug bioactivation in drug discovery and development. *Chem. Res. Toxicol. 17*, 3–16.
(18) Ju, C., and Uetrecht, J. P. (2002) Mechanism of idiosyncratic drug reactions: reactive metabolite formation, protein binding and the regulation of the immune system. *Curr. Drug Metab. 3*, 367–377.
(19) Dalvie, D. K., Kalgutkar, A. S., Khojasteh-Bakht, S. C., Obach, R. S., and O'Donnell, J. P. (2002) Biotransformation reactions of five-membered aromatic heterocyclic rings. *Chem. Res. Toxicol. 15*, 269–299.
(20) Mizutani, T., Yoshida, K., and Kawazoe, S. (1994) Formation of toxic metabolites from thiabendazole and other thiazoles in mice. Identification of thioamides as ring cleavage products. *Drug Metab. Dispos. 22*, 750–755.
(21) Mizutani, T., and Suzuki, K. (1996) Relative hepatotoxicity of 2-(substituted phenyl)thiazoles and substituted thiobenzamides in mice: evidence for the involvement of thiobenzamides as ring cleavage metabolites in the hepatotoxicity of 2-phenylthiazoles. *Toxicol. Lett. 85*, 101–105.
(22) Stevens, G. J., Hitchcock, K., Wang, Y. K., Coppola, G. M., Versace, R. W., Chin, J. A., Shapiro, M., Suwanrumpha, S., and Mangold, B. L. (1997) In vitro metabolism of *N*-(5-chloro-2-methylphenyl)-*N*′-(2-methylpropyl)thiourea: species comparison and identification of a novel thiocarbamide-glutathione adduct. *Chem. Res. Toxicol. 10*, 733–741.
(23) Kedderis, G. L., and Miwa, G. T. (1988) The metabolic activation of nitroheterocyclic therapeutic agents. *Drug Metab. Rev. 19*, 33–62.
(24) Lakshmi, V. M., Zenser, T. V., Sohani, S., and Davis, B. B. (1992) Mechanism of formation of the thioether conjugate of the bladder carcinogen 2-amino-4-(5-nitro-2-furyl)-thiazole (ANFT). *Carcinogenesis 13*, 2087–2093.
(25) Lakshmi, V. M., Mattammal, M. B., Zenser, T. V., and Davis, B. B. (1990) Mechanism of peroxidative activation of the bladder carcinogen 2-amino-4-(5-nitro-2-furyl)-thiazole (ANFT): comparison with benzidine. *Carcinogenesis 11*, 1965–1970.
(26) Blumberg, L. C., Brown, M. F., Munchhof, M. J., and Reiter, L. A. (2007) Aminothiazole derivatives as agonists of the thrombopoietin receptor. WO2007004038 A1.
(27) Blumberg, L. C., Brown, M. F., Munchhof, M. J., and Reiter, L. A. (2007) Aminothiazole derivatives as agonists of the thrombopoietin receptor. WO2007036769 A1.
(28) Paul, S., Gupta, M., and Loupy, A. (2002) Microwave assisted synthesis of 1,5-disubstituted hydantoins and thiohydantoins in solvent-free conditions. *Synthesis 1*, 75–78.
(29) Xu, X., Yang, Z., Chen, G., and Qian, X. (2003) A facile synthesis of substituted *N*-benzoylthiourea. *Synth. Commun. 33*, 2585–2592.
(30) Benet, L. Z., and Galeazzi, R. L. (1971) Noncompartmental determination of the steady-state volume of distribution. *J. Pharm. Sci. 68*, 1071–1074.
(31) Baillie, T. A., and Davis, M. R. (1993) Mass spectrometry in the analysis of glutathione conjugates. *Biol. Mass Spectrom. 22*, 319–325.
(32) Kulanthaivel, P., Barbuch, R. J., Davidson, R. S., Yi, P., Rener, G. A., Mattiuz, E. L., Hadden, C. E., Goodwin, L. A., and Ehlhardt, W. J. (2004) Selective reduction of *N*-oxides to amines: application to drug metabolism. *Drug Metab. Dispos. 32*, 966–972.
(33) Thomas, R. C., and Harpootlian, H. (1975) Metabolism of minoxidil, a new hypotensive agent II: biotransformation following oral administration to rats, dogs, and monkeys. *J. Pharm. Sci. 64*, 1366–1371.
(34) Nelson, S. D., Nelson, W. L., and Trager, W. F. (1978) *N*-Hydroxyamide metabolites of lidocaine. Synthesis, characterization, quantitation, and mutagenic potential. *J. Med. Chem. 21*, 721–725.
(35) Zlokarnik, G., Negulescu, P. A., Knapp, T. E., Mere, L., Burres, N., Feng, L., Whitney, M., Roemer, K., and Tsien, R. Y. (1998) Quantitation of transcription and clonal selection of single living cells with β-lactamase as reporter. *Science 279*, 84–88.
(36) Hobbs, D. C., and Twomey, T. M. (1977) Metabolism of sudoxicam by the rat, dog, and monkey. *Drug Metab. Dispos. 5*, 75–81.
(37) Rainsford, K. D. (2004) Pharmacology and toxicology of COX-2 inhibitors. In *COX-2 Inhibitors/Milestones in Drug Therapy* (Pairet, M., and van Ryn, J., Eds.) pp 67–132, Birkhauser, Basel, Switzerland.
(38) Chesne, C., Guyomard, C., Guillouzo, A., Schmid, J., Ludwig, E., and Sauter, T. (1998) Metabolism of Meloxicam in human liver involves cytochromes P4502C9 and 3A4. *Xenobiotica 28*, 1–13.
(39) Hobbs, D. C., and Twomey, T. M. (1981) Metabolism of piroxicam by laboratory animals. *Drug Metab. Dispos. 9*, 114–118.
(40) Voogd, C. E., van der Stel, J. J., and Verharen, H. W. (1983) The capacity of some nitro- and amino-heterocyclic sulfur compounds to induce base-pair substitutions. *Mutat. Res. 118*, 153–165.
(41) Rice, J. R., Zenser, T. V., and Davis, B. B. (1985) Formation of thioether conjugates of the bladder carcinogen ANFT catalyzed by prostaglandin synthase. *Carcinogenesis 6*, 585–590.
(42) Musah, R. A., and Goodin, D. B. (1997) Introduction of novel substrate oxidation into cytochrome *c* peroxidase by cavity complementation: oxidation of 2-aminothiazole and covalent modification of the enzyme. *Biochemistry 36*, 11665–11674.
(43) Bessems, J. G. M., de Groot, M. J., Baede, J. M., te Koppele, J. M., and Vermeulen, N. P. E. (1998) Hydrogen atom abstraction of 3,5-disubstituted analogues of paracetamol by horseradish peroxidase and cytochrome P450. *Xenobiotica 28*, 855–875.
(44) Kassahun, K., Skordos, K., McIntosh, I., Slaughter, D., Doss, G. A., Baillie, T. A., and Yost, G. S. (2005) Zafirlukast metabolism by cytochrome P450 3A4 produces an electrophilic α,β-unsaturated iminium species that results in the selective mechanism-based inactivation of the enzyme. *Chem. Res. Toxicol. 18*, 1427–1437.
(45) Yang, X., and Chen, W. (2005) In vitro microsomal metabolic studies on a selective mGluR5 antagonist MTEP: characterization of in vitro metabolites and identification of a novel thiazole ring opening aldehyde metabolite. *Xenobiotica 35*, 797–809.
(46) Offen, C. P., Frearson, M. J., Wilson, K., and Burnett, D. (1985) 4,5-Dimethylthiazole-*N*-oxide-*S*-oxide: a metabolite of chlormethiazole in man. *Xenobiotica 15*, 503–511.
(47) Testa, B., and Mayer, J. M. (2003) The hydrolysis of amides. In *Hydrolysis in Drug and Prodrug Metabolism (Chemistry, Biochemistry, and Enzymology)* (Testa, B., and Mayer, J. M., Eds.) Chapter 4, pp 81–162, VHCA, Zürich.
(48) Spahn-Langguth, H., and Benet, L. Z. (1992) Acyl glucuronides revisited: is the glucuronidation process a toxification as well as a detoxification mechanism? *Drug Metab. Rev. 24*, 5–47.
(49) Shipkova, M., Armstrong, V. W., Oellerich, M., and Wieland, E. (2003) Acyl glucuronide drug metabolites: toxicological and analytical implications. *Ther. Drug Monit. 25*, 1–16.
(50) Benet, L. Z., Spahn-Langguth, H., Iwakawa, S., Volland, C., Mizuma, T., Mayer, S., Mutschler, E., and Lin, E. T. (1993) Predictability of the covalent binding of acidic drugs in man. *Life Sci. 53*, PL141–PL146.
(51) Bolze, S., Bromet, N., Gay-Feutry, C., Massiere, F., Boulieu, R., and Hulot, T. (2002) Development of an in vitro screening model for the biosynthesis of acyl glucuronide metabolites and the assessment of their reactivity toward human serum albumin. *Drug Metab. Dispos. 30*, 404–413.
(52) Castillo, M., and Smith, P. C. (1995) Disposition and reactivity of ibuprofen and ibufenac acyl glucuronides in vivo in the rhesus monkey and in vitro with human serum albumin. *Drug Metab. Dispos. 23*, 566–572.

TX700270R